Oral presentation | Turbulence simulation (DNS,LES,RANS)
Turbulence simulation(DNS,LES,RANS)-II
Wed. Jul 17, 2024 4:30 PM - 6:30 PM Room B

[9-B-04] High-Fidelity Simulations of Active Flow Control Over An Airfoil With Deep Reinforcement Learning

*Kevin Tan[1], Kengo Asada[1], Tomoaki Tatsukawa[1], Kozo Fujii[1] （1. Department of Information and Computer Technology, Tokyo University of Science）

Keywords: DBD Plasma Actuators, Deep Reinforcement Learning, Large-eddy simulation, airfoil stall, NACA0015

Twelfth International Conference on
Computational Fluid Dynamics (ICCFD12),
Kobe, Japan, July 14-19, 2024

High-Fidelity Simulations of Active Flow Control Over an Airfoil With Deep Reinforcement Learning

Kevin Tan*, Kengo Asada*, Tomoaki Tatsukawa*, and Kozo Fujii*
Corresponding author: 4623517@ed.tus.ac.jp
* Tokyo University of Science, Japan.

1 Introduction

Recently, DBD plasma actuators (PA) [1] have been actively studied as microflow control devices for suppressing separated flows around airfoils. Burst actuation, whose driving condition is determined by the nondimensional burst frequency (F^+), is demonstrated superior separation control capability compared to continuous actuation [2]. However, it is still difficult to determine the appropriate F^+ for varying flow conditions. Shimomura et al. [3] attempted to determine an appropriate burst driving method using the deep Q-network, which is a kind of Deep Reinforcement Learning (DRL)[4], through the experimental study and discovered effective driving strategies. In experiments, the information obtained regarding the flow fields is limited. On the other hand, it is possible to obtain more information by utilizing numerical simulation. This study aims to establish a high-fidelity simulation framework coupling DRL and confirm that the obtained flow control strategy achieves a better control capability than the conventional burst actuation.

2 Problem Statement

In the present study, we construct a simulation framework consisting of a DRL program and a CFD solver, which would be a new use case of supercomputers, as shown in Fig. 1. The DRL agent determines the optimal F^+ based on time series pressure data obtained from sensors on the airfoil surface. The reward is given according to the trailing edge pressure. Unlike experiments, high-fidelity simulations require much computational time, and the number of computation runs is limited. Thus, we use a higher learning rate than the experiment in the present study because the number of data used for training and updating the network is less. An in-house code, LANS3D [5], is used for fluid simulation, which has been developed by our research for many years. Flows around an NACA0015 airfoil are considered. The Reynolds number is set to 63,000, and the two angles of attack (12 and 15 degrees) are considered. Hereafter, we define the pressure coefficient, freestream speed, chord length, and nondimensional time as C_p, U_∞, c, and t^+ ($= tU_\infty/c$), respectively.

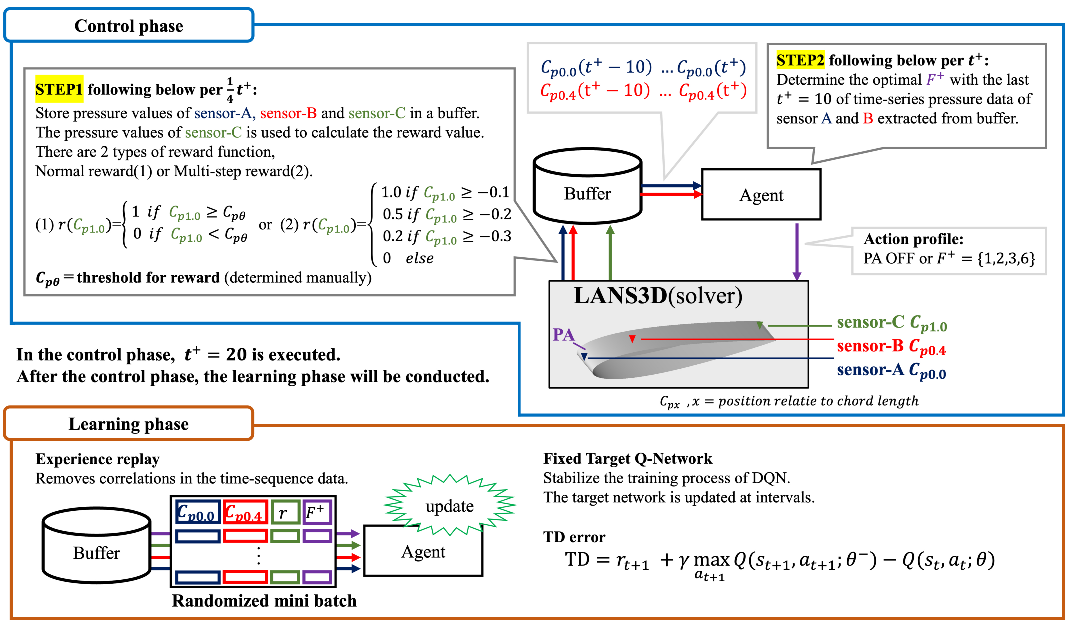

Figure 1: DRL based framework and procedures.

Table 1: Parameters of DRL in 12 degrees of Angle of Attack

	model-A	model-B
Mini-batch size	20	
Episode number	12	
Discount rate	0.99	
Max memory size	240	
Optimizer	Adam Optimizer	
Target network update interval	3	
Epsilon	$\varepsilon = 0.9 - 0.09\times$episode	descend from 0.9 to 0.1 like a sigmoid
Minimum of Epsilon	0.1	
Learning rate	0.01	descend from 0.015 to 0.01
Reward $C_{p\theta}$: threshold for reward $C_{p1.0}$: Pressure of sensor-C	Normal Reward $C_{p\theta}$ = -0.09 $r = \begin{cases} 1 \text{ if } C_{p1.0} \geq C_{p\theta} \\ 0 \text{ if } C_{p1.0} < C_{p\theta} \end{cases}$	Multi-step Reward $r = \begin{cases} 1.0 \text{ if } C_{p1.0} \geq -0.1 \\ 0.5 \text{ if } C_{p1.0} \geq -0.2 \\ 0.2 \text{ if } C_{p1.0} \geq -0.3 \\ 0.0 \text{ if } C_{p1.0} < -0.3 \end{cases}$

Table 2: Parameters of DRL in 15 degrees of Angle of Attack

	model-C	model-D
Mini-batch size	20	
Episode number	16	
Discount rate	0.99	
Max memory size	320	
Optimizer	Adam Optimizer	
Target network update interval	3	
Epsilon	descend from 0.9 to 0.1 like a sigmoid	
Learning rate	descend from 0.015 to 0.001	
Reward $C_{p\theta}$: threshold for reward $C_{p1.0}$: Pressure of sensor-C	Multi-step Reward $r = \begin{cases} 1.0 \text{ if } C_{p1.0} \geq -0.1 \\ 0.5 \text{ if } C_{p1.0} \geq -0.2 \\ 0.2 \text{ if } C_{p1.0} \geq -0.3 \\ 0.0 \text{ if } C_{p1.0} < -0.3 \end{cases}$	Normal Reward $C_{p\theta}$ = -0.15 $r = \begin{cases} 1 \text{ if } C_{p1.0} \geq C_{p\theta} \\ 0 \text{ if } C_{p1.0} < C_{p\theta} \end{cases}$

In the present study, we performed four computational cases with different DRL models: models A and B for the angles of attack of 12 degrees and models C and D for 15 degrees. The learning parameters for each are shown in Tables 1 and 2.

3 Results

Figure 2 shows the history of pressure coefficient at the trailing edge ($C_{p1.0}$), which is used to calculate immediate reward. The horizontal axis is t^+, and the pressure history of all episodes is shown here. When the $C_{p1.0}$ value is above the threshold, the model's agent is rewarded. As the episodes progress, the agent learns to make the trailing edge pressure exceed the threshold. Fig. 3 shows the time histories of the lift-drag ratio and the selected F^+ by the DRL network. As learning progressed, the agent preferentially selected $F^+ = 6$, and the lift-drag ratio improved. The burst actuation with $F^+ = 6$ is known as an effective burst frequency by the previous parametrical study by Sato et al. [6]. These results show the present DRL network automatically found the optimal burst frequency without prior knowledge.

Figures 4 and 5 show the lift and drag coefficients of the model-C and model-D. Separation control is difficult at the angle of attack 15 degrees by a fixed F^+. The model-C converges to selecting $F^+ = 2$, while model-D does not. Both models cannot obtain stable lift and drag coefficients. However, the duration, where the lift temporally improved, is seen at $t^+ \simeq 6 - 8$ at the 12th episode of model-D. At this duration, the nested burst actuation, such as repeating the sequence of actuating PA in burst for a certain t^+ and then turning the PA off for a certain t^+ is seen. This is similar to the results shown in the previous study by Shimomura et al.[3].

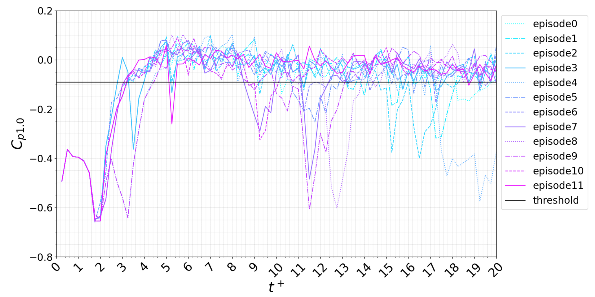

Figure 2: History of pressure coefficient at the trailing edge of model-A.

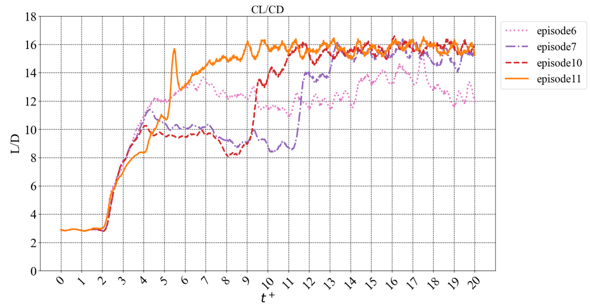

(a) Lift-to-drag ratio

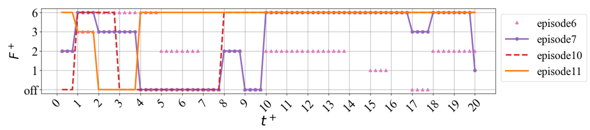

(b) Action history

Figure 3: histories of lift-to-drag ratio and action history, the model-A.

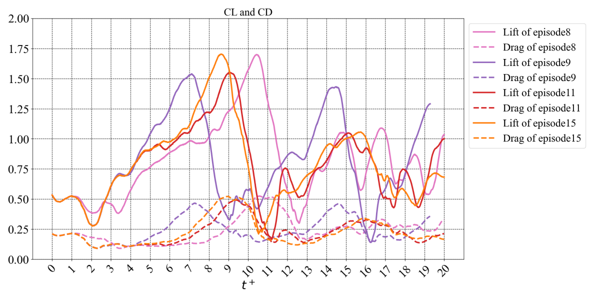

(a) Lift and drag coefficients

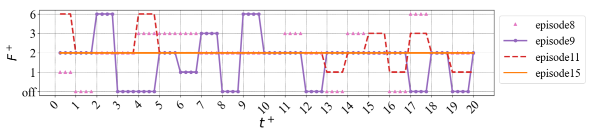

(b) Action history

Figure 4: Lift and drag histories of model-C.

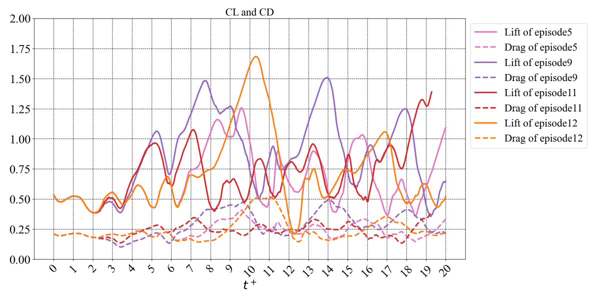

(a) Lift and drag coefficients

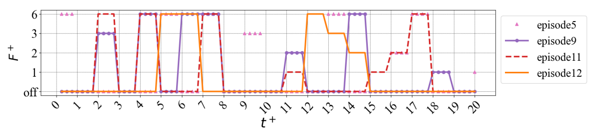

(b) Action history

Figure 5: Lift and drag histories of model-D.

Figure 6 shows the instantaneous flow fields for 12th episode of the model-D in the duration of the nested burst actuation. The iso-surface is the second invariant of the velocity gradient tensor colored by the chordwise velocity (u/U_∞). The flow at $t^+ = 4$ (Fig. 6(a)) is separated. However, when the nested burst actuation starts at $t^+ \simeq 5$, the large-scale vortices are generated by PA, and the separated shear-layer is entrained to the airfoil surface as shown in Fig. 6(b). After that, the separated region is reduced at $t^+ = 8$ (Fig. 6(c)), and after three non-dimensional time elapsed since PA turned off (t=7), the flow is largely separated again as shown in Fig. 6(d). Although the present learned model can not stably suppress the separation area, the model could achieve a higher lift coefficient if it properly learns and utilizes the nested burst actuation.

The present study established the simulation framework that combines the high-fidelity simulation (LES) and the Deep Reinforcement Learning (DRL) to conduct feedback flow separation control around the airfoil using a burst actuation of the PA. At the angle of attack of 12 degrees, the burst drive with $F^+ = 6$ was selected by DRL agent, similar to the experimental study [3], and it was shown that flow separation can be suppressed. At the angle of attack 15 degrees, the DRL models temporarily improve

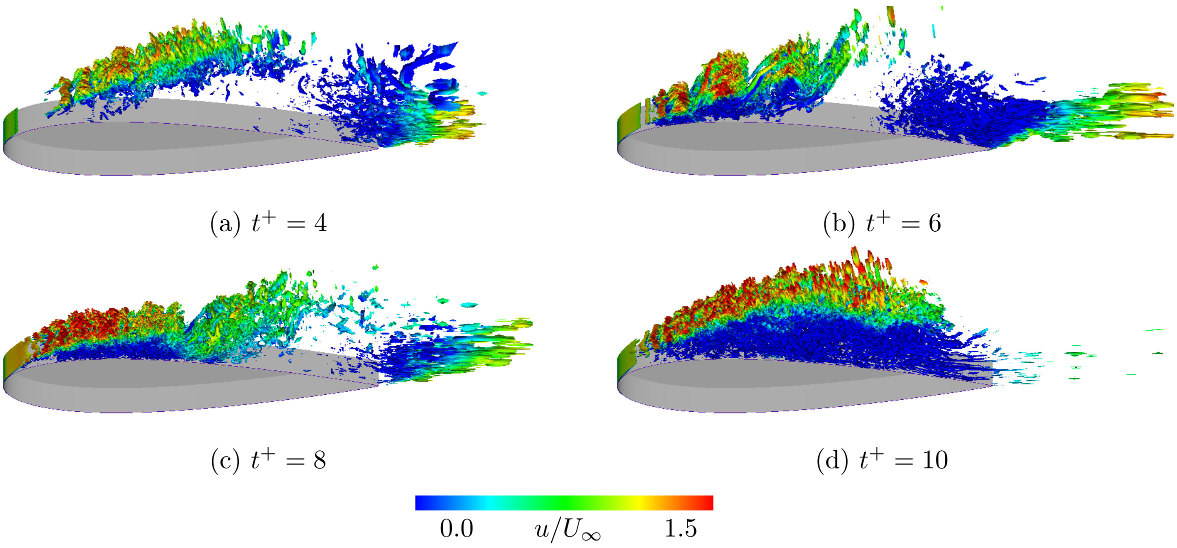

(a) $t^+ = 4$ (b) $t^+ = 6$

(c) $t^+ = 8$ (d) $t^+ = 10$

Figure 6: Instantaneous flow of the model-D, 12th episode.

the lift coefficient. At the lift improved duration, the agent of the model-D produced a characteristic control history, such as the nested burst actuation.

4 Acknowledgement

I would like to acknowledge the support of the Cyber Science Center at Tohoku University (Project code : kyo017), for their support of this work. This study has been supported in part by Grant-in-aid KAKENHI (22 K04536).

References

[1] J. R. Roth, D. M. Sherman, and S. P. Wilkinson. Electrohydrodynamic flow control with a glow-discharge surface plasma. *AIAA Journal*, 38(7):1166–1172, 2000.

[2] S. Sekimoto, T. Nonomura, and K. Fujii. Burst-mode frequency effects of dielectric barrier discharge plasma actuator for separation control. *AIAA Journal*, 55(4):1385–1392, 2017.

[3] S. Shimomura, S. Sekimoto, A. Oyama, K. Fujii, and H. Nishida. Closed-loop flow separation control using the deep q network over airfoil. *AIAA Journal*, 58(10):4260–4270, 2020.

[4] V. Mnih, K. Kavukcuoglu, D. Silver, A. A. Rusu, J. Veness, M. G. Bellemare, A. Graves, M. A. Riedmiller, A. K. Fidjeland, G. Ostrovski, S. Petersen, C. Beattie, A. Sadik, I. Antonoglou, H. King, D. Kumaran, D. Wierstra, S. Legg, and D. Hassabis. Human-level control through deep reinforcement learning. *Nature*, 518:529–533, 2015.

[5] K. Fujii and Y. Tamura. Capability of current supercomputers for the computational fluid dynamics. In *Proceedings of the 1989 ACM/IEEE Conference on Supercomputing*, Supercomputing '89, page 71–80, New York, NY, USA, 1989. Association for Computing Machinery.

[6] M. Sato, H. Aono, A. Yakeno, T. Nonomura, K. Fujii, K. Okada, and K. Asada. Multifactorial effects of operating conditions of dielectric-barrier-discharge plasma actuator on laminar-separated-flow control. *AIAA journal*, 53(9):2544–2559, 2015.